



# UNIVERSITÀ DI PARMA

## ARCHIVIO DELLA RICERCA

University of Parma Research Repository

Characterisation of SnSe thin films fabricated by chemical molecular beam deposition for use in thin film solar cells

This is a pre print version of the following article:

*Original*

Characterisation of SnSe thin films fabricated by chemical molecular beam deposition for use in thin film solar cells / Razykov, T. M.; Boltaev, G. S.; Bosio, A.; Ergashev, B.; Kouchkarov, K. M.; Mamarasulov, N. K.; Mavlonov, A. A.; Romeo, A.; Romeo, N.; Tursunkulov, O. M.; Yuldoshov, R.. - In: SOLAR ENERGY. - ISSN 0038-092X. - 159:(2018), pp. 834-840. [10.1016/j.solener.2017.11.053]

*Availability:*

This version is available at: 11381/2838575 since: 2021-10-04T09:31:48Z

*Publisher:*

Elsevier Ltd

*Published*

DOI:10.1016/j.solener.2017.11.053

*Terms of use:*

Anyone can freely access the full text of works made available as "Open Access". Works made available

*Publisher copyright*

note finali coverpage

(Article begins on next page)

# Characterisation of SnSe thin films fabricated by chemical molecular beam deposition for use in thin film solar cells

T.M.Razykov<sup>1</sup>, G.S. Boltaev<sup>2</sup>, A.Bosio<sup>3</sup>, B.Ergashev<sup>1</sup>, K.M.Kouchkarov<sup>1</sup>,  
N.K. Mamarasulov<sup>1</sup>, A.A. Mavlonov<sup>1</sup>, A.Romeo<sup>4</sup>, N.Romeo<sup>3</sup>, R.Yuldoshov<sup>1</sup>

<sup>1</sup>Physical-Technical Institute, Uzbekistan Academy of Sciences,  
Bodomzor Yoli 2B, Tashkent 100084, Uzbekistan

Phone: +998-71-235-4103, Fax: +998-71-235-4291, E-mail: [razykov@uzsci.net](mailto:razykov@uzsci.net)

<sup>2</sup>Ion Plasma and Laser Technologies, Uzbek Academy of Sciences, Tashkent 100125, Uzbekistan

<sup>3</sup>University of Parma, G.P Usberti 7/A - 43124 Parma, Italy

<sup>4</sup>Universita' di Verona, Ca' Vignal 2- Strada Le Grazie 15, 37134 Verona, Italy

## ABSTRACT

SnSe thin films were fabricated the first time by chemical molecular beam deposition (CMBD) in atmospheric pressure hydrogen flow using polycrystalline tin selenium (SnSe) precursors. The morphological and electrical properties of the films were studied as a function of the precursor's composition and the substrate temperature. Experimental data indicate that in the resulting thin films Se enrichment takes place at low substrate temperatures, despite the different compositions of the SnSe precursor during the synthesis. In this case, the grain sizes of the films vary in the range of 8-20  $\mu\text{m}$ , depending on the substrate temperature. In addition, X-ray diffraction analysis of the samples shows that the films have an orthorhombic crystalline structure. The electrical conductivity of films measured by van der Pauw method varies between 6 and 90 ( $\Omega \times \text{cm}$ )<sup>-1</sup>. The optical measurements on selected SnSe thin films illustrate that the sample has an optical bandgap of 1.21 eV and the absorption coefficient of  $\sim 10^5 \text{ cm}^{-1}$ .

**Keywords:** thin film, SnSe, chemically molecular beam deposition, X-ray diffraction, bandgap

## INTRODUCTION

Currently, the leading materials in the world photovoltaic (PV) market are silicon (Si) with an efficiency of 25%, Cu(In,Ga)Se<sub>2</sub> (CIGSe) - 22.6% [1, 2] and CdTe -22.1% [3, 4].

Despite the wide use of these compounds, there are significant limitations in their use in the global production of PV modules. For example, the main disadvantage of Si-based solar cells is that Si does not have the optimal bandgap (1.1 eV) and has a low absorption coefficient ( $\sim 10^2 \text{ cm}^{-1}$ ), which increases the material cost, since it is required to use the material with a minimum thickness of 100-200  $\mu\text{m}$  [5]. At the same time, further large-scale applications for thin-film solar cells based on CIGSe and CdTe materials are complicated because of the limited In, Ga, Te in the earth's crust, as well as the toxicity issues of Cd [6].

Proceeding from this, many research centers and laboratories have aimed to replace these expensive materials of In and Ga with Zn and Sn elements in CIGSe as the main optical properties of these materials are suggested to be unaffected. The main advantages of these elements are their low cost (prevalence in nature) and non-toxicity. To date, the efficiency of solar cells based on Cu<sub>2</sub>ZnSnS<sub>x</sub>Se<sub>4-x</sub> (CZTSe) is 12.6%. So far, this data was obtained in IBM's research center and is the maximum for the last 20 years [7]. As CZTSSe belongs to a quaternary system, the precise control of composition and structural transitions is difficult due to more number of elements [8]. Moreover, too many elements in

this absorber may also increase the production cost of the solar cells. Therefore, in view of mass production at lower cost, the use of both CIGSe and CZTSe will be limited in the near future.

Tin-based binary semiconductors, such as SnS and SnSe are expected to play a crucial role in replacing the above technologies in the near future owing to their relatively earth-abundance, non-toxic nature, and easy controllability of stoichiometry.

These materials exhibit favorable properties, such as high chemical stability, suitable band gap (1.0 eV -1.5 eV), and high absorption coefficient ( $\sim 10^5 \text{ cm}^{-1}$ ) with *p*-type conductivity [11-14]. In addition, they show a maximum theoretical efficiency of 33% [15]. Therefore, these materials have great potential to replace the toxic (CdTe) and scarce elements based (CIGS) absorbers in photovoltaic devices. On the other hand, the solar cells fabricated from these materials (SnS and SnSe) currently exhibited lower efficiencies ( $\leq 1\%$  by non-vacuum methods and  $<5\%$  by vacuum methods) than CIGS and CZTS solar cells. The lower efficiency has been attributed to a lack of precise control over the pure phase formation and fine-tuning of the band gap by the adopted technology. In thermal growth methods, owing to high volatility of sulfur, it is very difficult to maintain the 1:1 ratio of Sn:S [16]. The sulfur deficiency can lead to the tin migration to grain boundaries, surfaces, interfaces, interstitial sites, or sulfur anti-sites [16]. In addition, the problem of a good heterojunction partner has not been fully rectified. All aforementioned issues can strongly influence the recombination losses at the device level [16].

To obtain SnSe thin films, various growth methods such as thermal evaporation [11], chemical vapor deposition [12, 13] electrodeposition [14], spray pyrolysis [15], magnetron sputtering [16] and others are used. The physical characteristics of the films, i.e. the optical bandgap, the direction and degree of preferential growth orientation, the phase of elemental composition, strongly depend on the growth conditions. In most cases, additional heat treatment (post-annealing) is required to obtain the resulting films with the optimal characteristics for their effective usage in thin-film solar cells.

The purpose of this work is to obtain SnSe thin films by technologically simple CMBD method, i.e. does not require subsequent annealing [17-19] and to study their physical properties as a function of growth conditions.

## EXPERIMENTAL

Polycrystalline SnSe precursors with the following proportions were used as source materials: 1) Sn-50 wt.% and Se-50 wt.%; 2) Sn-50.7 wt.% and Se 49.3 wt.%; 3) Sn-40 wt.% and Se-60 wt.%. The SnSe precursors were obtained as follows: the Sn and Se elements were placed in quartz ampoules in which a vacuum was created. Subsequently, quartz ampoules were loaded into a furnace and heated at 880 °C for 72 hours in order to synthesize SnSe compounds. Finally, quartz ampoules were cooled to room temperature (RT). In order to check whether SnSe compounds were formed, X-ray diffraction (XRD) measurements were performed. XRD analysis shows that SnSe compounds were formed which have an orthorhombic crystal structure.

The preparation of a polycrystalline SnSe thin film was carried out according to the procedure described in [20]. The evaporator was loaded with SnSe precursor and it was put into the growth chamber and purged with hydrogen in order to remove atmospheric pollutants from it. Subsequently, the outer furnace of the chamber was turned on. The heating level is determined by the set deposition temperatures. When the substrate is has reached the required temperature, the individual heater (A4B6) is turned on in order to adjust the evaporator temperature to the required temperature. The temperature of evaporation was established to be in the range of (850 ÷ 950) °C, and the temperature of the substrate was varied between 450°C-550°C. The flow rate of the carrier gas was  $\sim 20 \text{ cm}^3 / \text{min}$ . The duration of the deposition process depends on the required film thickness and ranges between (30 ÷ 60) min. All SnSe thin films have been grown on borosilicate glasses.

The crystal structure and the phase of the material compositions were studied by XRD using a "Panalytical Empyrean" diffractometer (CuK $\alpha$  radiation,  $\lambda = 1.5418 \text{ \AA}$ ) with a wide-angle

measurements of  $2\theta$  in the range of  $(20 \div 80)^\circ$  and a step of  $0.01^\circ$ . The experimental data were analyzed using the Joint Committee on Powder Diffraction Standard (JCPDS). Morphological studies were carried out using a scanning electron microscope (SEM-EVO MA 10), and film compositions were determined using an energy-dispersive X-ray spectroscopy (EDX, Oxford Instrument - Aztec Energy Advanced X-act SDD).

Optical parameters of selected SnSe thin film were determined from the transmission spectra obtained in a wide spectral range between  $(400 \div 2500)$  nm using the HR 4000 Ocean Optic spectrometer with a resolution of 2 nm.

For electrical measurements, ohmic contacts were realized by vacuum deposition of metals on as-deposited films. Silver was used as an ohmic contact. The type of conductivity of the samples was determined by thermoelectric effect. The thickness of the films ( $1\text{-}3\ \mu\text{m}$ ) was determined using microinterferometer MII-4, and the method of precision micro-weighting (on FA 120 4C scales with an accuracy of 0.1 mg).

## RESULTS AND DISCUSSION

According to EDX data, the obtained films do not have any impurity elements within the sensitivity of the method (cf. Figure 1). The deposited films from the Sn enriched SnSe precursor have an almost similar, stoichiometric composition at substrate temperatures of  $450^\circ\text{C}$  and  $500^\circ\text{C}$ . On the other hand, the film grown at  $550^\circ\text{C}$  has Sn enriched composition. This can be explained by the fact that when the substrate temperature increases, Se re-evaporates from the substrate, which results in enrichment of the Sn in the films [21]. All films deposited from the SnSe precursors enriched with Se and stoichiometric composition, yielded Se enriched composition in the films at different temperatures (cf. Table 1). All SnSe films studied in this work have a smooth surface without cracks and pores on the surface of the substrate. Thermoelectric studies depict that all SnSe films exhibit a *p*-type conductivity.

Figure 2 shows the XRD patterns of SnSe films deposited from three different SnSe precursors, i.e. Sn enriched, Se enriched and with stoichiometric composition, for three different substrate temperatures. According to XRD analysis, all thin films showed single-phase, the orthorhombic structure of SnSe and there are no other crystalline phases of Sn, Se,  $\text{Sn}_2\text{Se}_3$ ,  $\text{SnSe}_2$ ,  $\text{SnO}_2$ , etc. As depicted, the main peaks are corresponding to the (400) and (111) preferential orientation of SnSe. A similar result was also noted in several works devoted to SnSe films obtained by thermal evaporation and chemical vapor deposition [11, 12]. The authors ascribe the presence of both (400) and (111) preferential orientations to the growth conditions, e.g. substrate temperature, the distance between the substrate and the target. In this work, (111) plane was observed only for SnSe thin films deposited from Sn enriched SnSe precursor at  $550^\circ\text{C}$  (cf. Figure 2a). Analyzing the XRD data of all samples with a database (JCPDS: 01-089-0233) showed that all films have an orthorhombic structure. In addition to these strong (400) and (111) peaks, (200), (201), (111), (410), (411), (600), (101), (011), (400), (020), (511), and (800) small peaks are also present, although their intensity was extremely small compared to the intensities of the (400) and (111) peaks.

The lattice parameters of the crystal for all samples were calculated using the following formula:  $1/d^2 = h^2/a^2 + k^2/b^2 + l^2/c^2$ , where  $d$  is the distance between the planes,  $h$ ,  $k$ ,  $l$  are Miller indices and  $a$ ,  $b$ ,  $c$  are lattice constants. The lattice constants for thin films deposited at different substrate temperatures from Sn and Se enriched and stoichiometric SnSe precursors have the following values:  $a = 11.52\text{\AA}$ ,  $b = 4.16\text{\AA}$ ,  $c = 4.43\text{\AA}$  and  $a = 11.48\text{\AA}$ ,  $b = 4.17\text{\AA}$ ,  $c = 4.39\text{\AA}$ , respectively. These values are in good agreement with the JCPDS database, as well as the data presented in the literature for SnSe thin films grown by various methods [14, 22]. Detailed structural parameters of all films are presented in Table 3.

Figure 3 illustrates SEM images for all samples grown at different substrate temperatures from Sn and Se enriched as well as stoichiometric SnSe precursors. Although the microcrystals for all SnSe

films are uniformly distributed over the film surface, the microstructure (shape and grain size) of the samples depends on both the substrate temperature and the precursor composition. With increasing the substrate temperature, the shape of the grains changes, whereas the grain sizes do not change significantly for the films deposited from Sn enriched SnSe precursor (cf. Figure 3a), and vice versa for the samples obtained from Se enriched and stoichiometric SnSe precursors. Furthermore, the grain shapes of all the samples have a flattened appearance for all substrate temperatures, except for films obtained from Sn enriched SnSe compound at a substrate temperature of 550 °C, which has the form of a parallelepiped. The samples obtained from Sn enriched precursor have similar grain sizes of 8–10 (8 ÷ 10) μm and have a polycrystalline structure for all substrate temperatures. However, the grain sizes of the films deposited from Se enriched and stoichiometric SnSe precursors increased, i.e. 8–20 (8 ÷ 20) μm, at the substrate temperature of 550 °C and the structure become more densely packed. Moreover, disappearance of vertically deposited grains on the surface of all SnSe films was observed with increasing the substrate temperature. The same results were also reported in [12].

The electrical parameters of the SnSe films, e.g conductivity  $\sigma$ , activation energy  $E_{ac}$  and the type of conductivity, are given in Table 2. As shown, all SnSe thin films exhibit *p*-type conductivity. The electrical conductivity of SnSe films deposited from Sn enriched SnSe precursor decreases with increasing the substrate temperature. This is explained by the increase of Sn content in the film deposited at high substrate temperature. Unlike, the electrical conductivity of those samples obtained from Se enriched and stoichiometric SnSe precursors increases with increasing the substrate temperature. This improvement is associated with an increase in the grain size and a decrease in the grain boundary density of the films grown at higher substrate temperatures [23].

Figure 4 shows Tauc plot, i.e.  $(\alpha hv)^2$  vs  $(hv)$ , for selected SnSe thin films with different composition grown at 400 °C and 450 °C. As shown, the optical bandgap of SnSe thin films has been determined to be in the range of (1.1 ÷ 1.2) eV in the Tauc plot using linear extrapolation of the leading edge. Since the plot of  $(\alpha hv)^2$  vs  $(hv)$  is almost linear, the direct nature of the optical transition in SnSe is confirmed. These obtained values are in good agreement with the reported data of those SnSe films prepared by various growth methods [11, 22].

## Conclusion

We have investigated the morphological, structural, optical and electrical properties of SnSe films for different substrate temperatures and composition.

It has been found that: 1) at low substrate temperatures, SnSe thin films are Se enriched, i.e. independent of the initial precursor composition; 2) with increasing the substrate temperature, foreign particles disappear from the film surfaces and the films have more closely packed polycrystalline structure; 3) the films have an orthorhombic structure and are characterized by preferential (400) and (111) plane orientations; 4) the electrical conductivity of the SnSe films deposited from Sn enriched precursor decreases with increasing the substrate temperature, whereas it increases in SnSe films obtained from the Se enriched and stoichiometric SnSe precursors. Further, optical measurements showed that all the samples SnSe thin films have a direct band gap of (1.1 ÷ 1.2) eV.

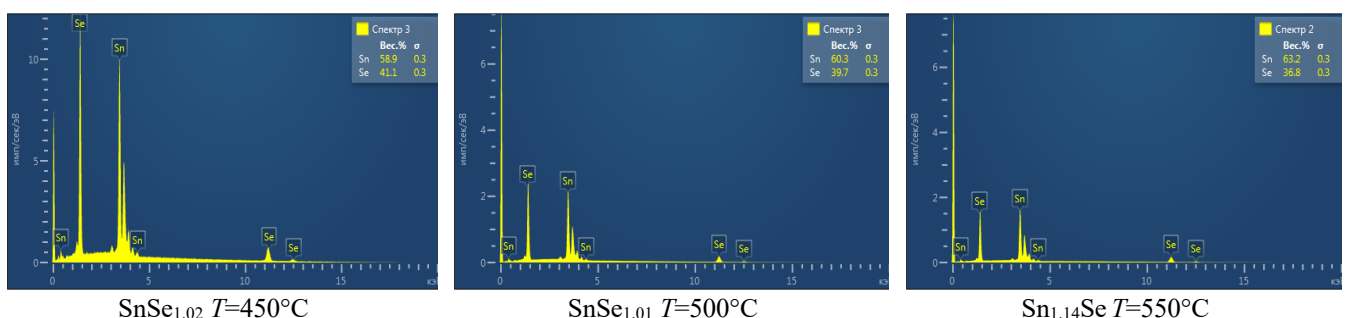


Figure 1. Results of energy dispersive X-ray spectroscopy analysis for SnSe thin films deposited from Sn enriched precursor at indicated substrate temperatures.

Table 1. Results of energy dispersive X-ray spectroscopy analysis for SnSe thin films deposited from Se enriched and stoichiometric SnSe precursors.  $T_s$  is the substrate temperature

$T_s$ (°C)	SnSe thin films deposited from stoichiometric SnSe precursor			SnSe thin films deposited from Se enriched SnSe precursor		
	Composition of the film	Sn%	Se%	Composition of the film	Sn%	Se%
450	Sn <sub>0.91</sub> Se	57.8	42.2	Sn <sub>0.89</sub> Se	57.3	42.7
500	Sn <sub>0.91</sub> Se	57.8	42.2	Sn <sub>0.96</sub> Se	59.2	40.8
550	Sn <sub>0.92</sub> Se	58.2	41.8	Sn <sub>0.95</sub> Se	58.7	41.3

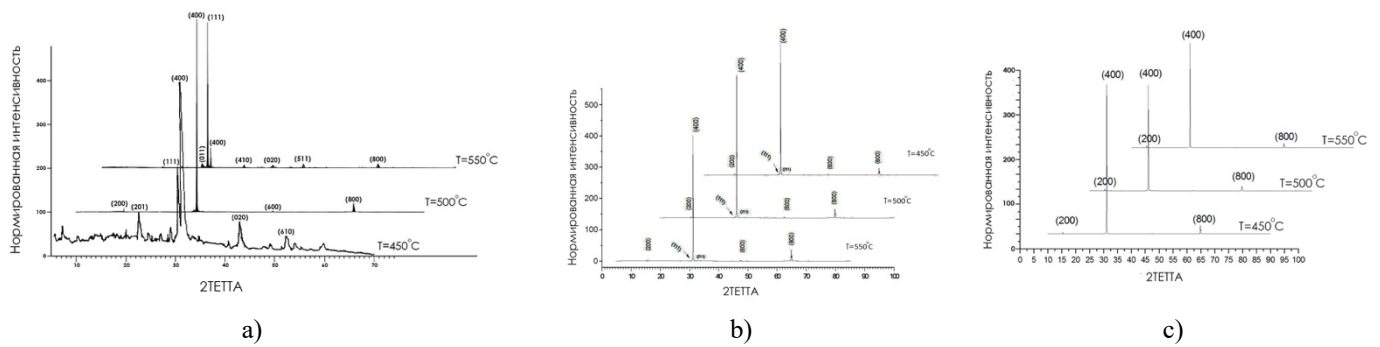


Figure 2. Wide-angle X-ray spectra of SnSe films obtained from a) Sn enriched, b) stoichiometric and c) Se enriched SnSe precursors at three different substrate temperatures.

Table 2. Electrical parameters of SnSe films.  $T_s$  -substrate temperature,  $\sigma$ -electrical conductivity,  $E_{ac}$ -activation energy

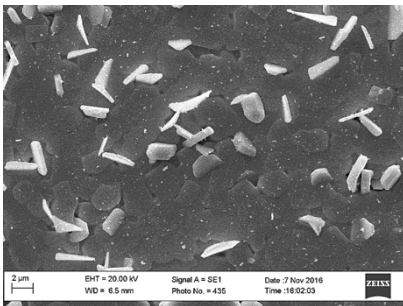
$T_s$ (°C)	SnSe thin films deposited from Sn enriched SnSe precursor				SnSe thin films deposited from stoichiometric SnSe precursor				SnSe thin films deposited from Se enriched SnSe precursor			
	Composition of the film	$\sigma$ (Ohm·cm) <sup>-1</sup>	$E_{ac}$ (eV)	Type of conductivity	Composition of the film	$\sigma$ (Ohm·cm) <sup>-1</sup>	$E_{ac}$ (eV)	Type of conductivity	Composition of the film	$\sigma$ (Ohm·cm) <sup>-1</sup>	$E_{ac}$ (eV)	Type of conductivity
450	Sn <sub>0.98</sub> Se	90	0.0023	<i>p</i>	Sn <sub>0.91</sub> Se	6,5	0.0023	<i>p</i>	Sn <sub>0.89</sub> Se	5,5	0.0022	<i>p</i>
500	Sn <sub>1.01</sub> Se	70	0.0024	<i>p</i>	Sn <sub>0.91</sub> Se	24	0.0025	<i>p</i>	Sn <sub>0.96</sub> Se	20	0.0024	<i>p</i>
550	Sn <sub>1.14</sub> Se	15	0.0406	<i>p</i>	Sn <sub>0.92</sub> Se	27	0.0026	<i>p</i>	Sn <sub>0.95</sub> Se	24	0.0028	<i>p</i>

Table 3. Structural parameters of SnSe films.  $(hkl)$ - Miller indices,  $d$ -the distance between the planes.

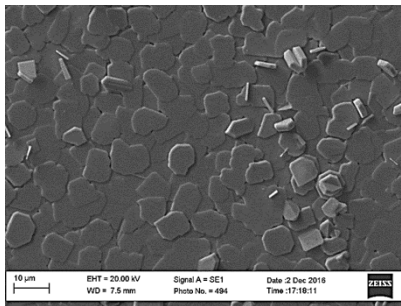
$T_s$ (°C)	SnSe thin films deposited from Sn enriched SnSe precursor				SnSe thin films deposited from stoichiometric SnSe precursor				SnSe thin films deposited from Se enriched SnSe precursor			
	Composition of the film	$2\theta$ (°)	$(hkl)$	$d$ (Å)	Composition of the film	$2\theta$ (°)	$(hkl)$	$d$ (Å)	Composition of the film	$2\theta$ (°)	$(hkl)$	$d$ (Å)
450	Sn <sub>0.98</sub> Se	25.3	(2 0 1)	3.72	Sn <sub>0.91</sub> Se	15.44	(2 0 0)	5.74	Sn <sub>0.89</sub> Se	15.40	(2 0 0)	5.74
		30.41	(1 1 1)	2.93		30.47	(1 1 1)	2.93		31.07	(4 0 0)	2.87
		31.02	(4 0 0)	2.88		31.11	(4 0 0)	2.87		64.7	(8 0 0)	1.44
		37.95	(0 2 0)	1.92		47.42	(6 0 0)	1.92				
		43.25	(6 1 0)	1.44		64.82	(8 0 0)	1.44				
		64.64	(8 0 0)	1.23								
500	Sn <sub>1.01</sub> Se	15.38	(2 0 0)	5.76	Sn <sub>0.91</sub> Se	15.45	(2 0 0)	5.73	Sn <sub>0.96</sub> Se	15.40	(2 0 0)	5.75



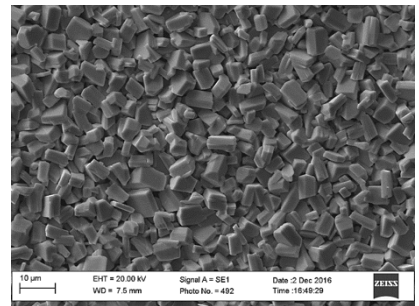
		30.43	(1 1 1)	2.93		30.46	(1 1 1)	2.93		31.07	(4 0 0)	2.87
		31.03	(4 0 0)	2.88		31.10	(4 0 0)	2.87		64.7	(8 0 0)	1.43
		47.31	(6 0 0)	1.92		47.39	(6 0 0)	1.92				
		64.68	(8 0 0)	1.44		64.78	(8 0 0)	1.44				
550	Sn <sub>1.14</sub> Se	21.42	(1 0 1)	4.15	Sn <sub>0.92</sub> Se	15.44	(2 0 0)	5.73	Sn <sub>0.95</sub> Se	15.40	(2 0 0)	5.74
		25.3	(2 0 1)	3.52		30.48	(1 1 1)	2.93		31.08	(4 0 0)	2.87
		29.41	(0 1 1)	3.03		31.11	(4 0 0)	2.87		64.78	(8 0 0)	1.44
		30.44	(1 1 1)	2.93		47.40	(6 0 0)	1.92				
		31.06	(4 0 0)	2.88		64.79	(8 0 0)	1.44				
		37.76	(4 1 0)	2.38								
		43.38	(0 2 0)	2.08								
		49.67	(5 1 1)	1.83								
		64.75	(8 0 0)	1.44								



Sn<sub>0.98</sub>Se  $T = 450^{\circ}\text{C}$

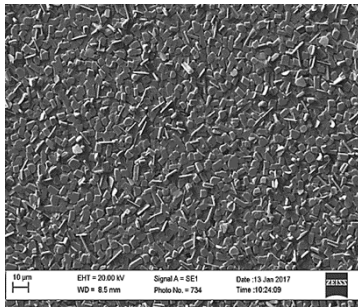


Sn<sub>1.01</sub>Se  $T = 500^{\circ}\text{C}$

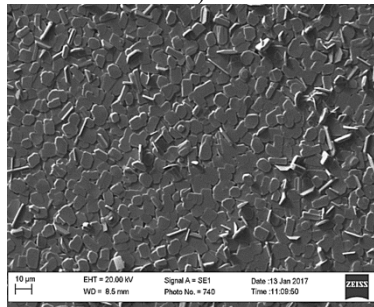


Sn<sub>1.14</sub>Se  $T = 550^{\circ}\text{C}$

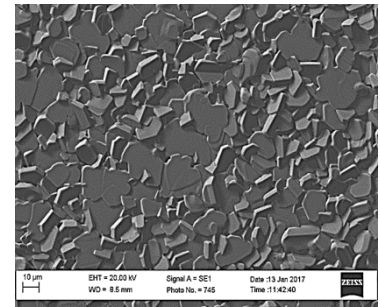
a)



Sn<sub>0.91</sub>Se  $T = 450^{\circ}\text{C}$

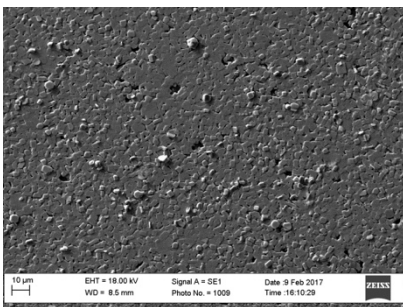


Sn<sub>0.91</sub>Se  $T = 500^{\circ}\text{C}$

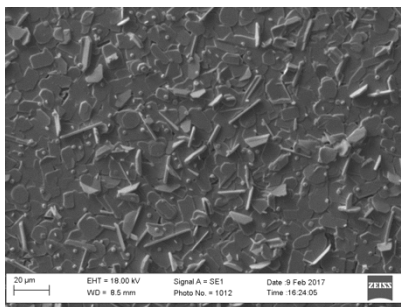


Sn<sub>0.92</sub>Se  $T = 550^{\circ}\text{C}$

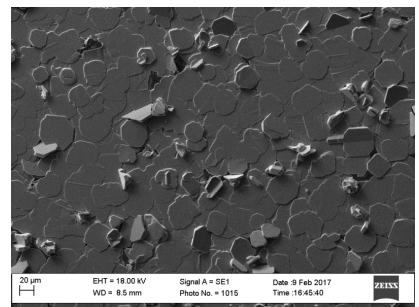
b)



Sn<sub>0.89</sub>Se  $T = 450^{\circ}\text{C}$



Sn<sub>0.96</sub>Se  $T = 500^{\circ}\text{C}$



Sn<sub>0.95</sub>Se  $T = 550^{\circ}\text{C}$

c)

Figure 3. SEM images of SnSe thin films deposited from a) Sn enriched, b) stoichiometric and c) Se enriched SnSe precursors at indicated substrate temperatures.

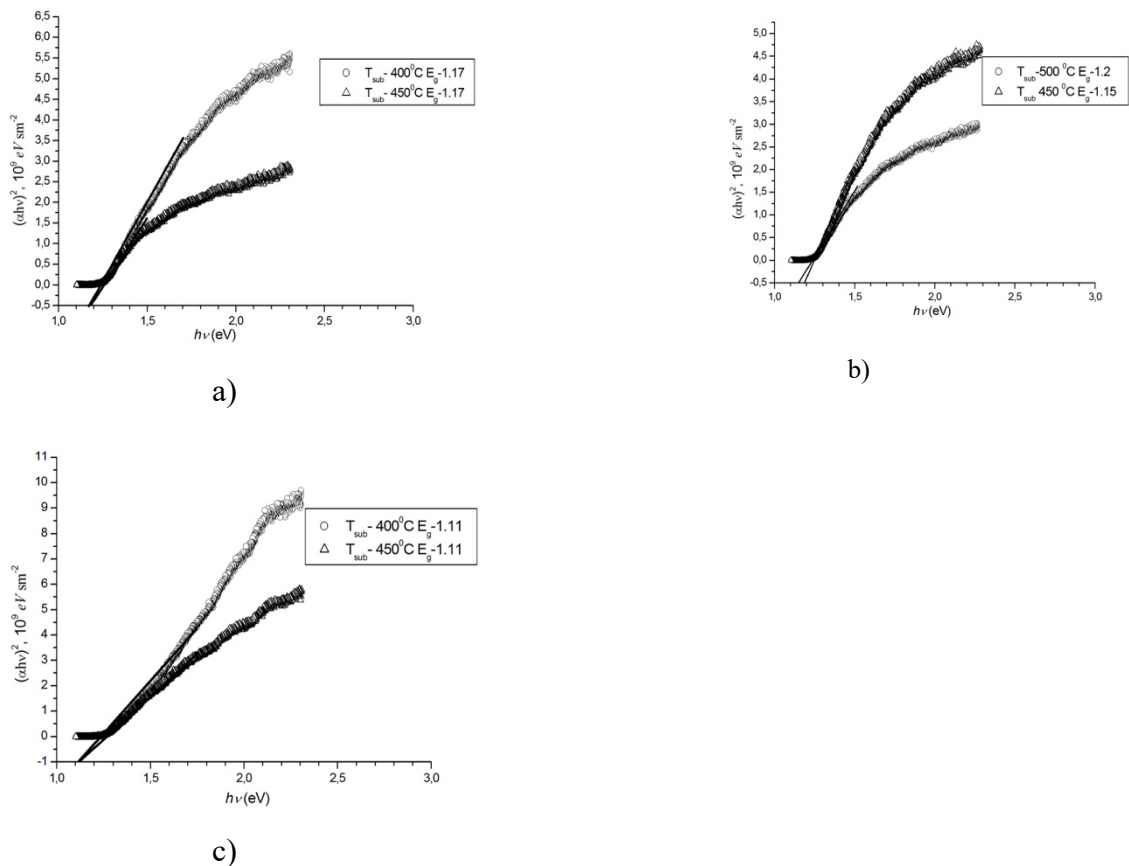


Figure 4. Absorption coefficient versus photon energy for SnSe thin films deposited from a) Sn enriched, b) stoichiometric and c) Se enriched SnSe precursors at two different substrate temperatures of 400 °C and 450°C.

## ACKNOWLEDGEMENT

The work was carried out within the framework of Fund for Supporting the Fundamental Research (Grant No. F.2-16) and Fundamental Research Project (Grant No. FA-F3-003).

<sup>1</sup>Physico-Technical Institute, Scientific Production Association "Physics-Sun", Uzbekistan Academy of Sciences

<sup>2</sup>Educational and Experimental Centre of High Technologies, Tashkent, Uzbekistan

## REFERENCES

- [1] Repins I, Contreras M. A, Egaas B, et. al. 19,9%-efficient ZnO/CdS/ CuInGaSe<sub>2</sub> solar cell with 81,2% fill factor. *Progress in Photovoltaics: Research and Applications* 2008; 16: 235–239.
- [2] Dr. Takuya Kato. Recent research progress of high-efficiency CIGS solar cell in Solar Frontier Solar Frontier (JPN), 7th International Workshop on CIGS Solar Cell Technology (IW-CIGSTech 7), 20 - 24 June 2016, ICM - International Congress Center Munich, Germany.
- [3] Wu X, Keane J. C, Dhare R. G, et. al. 16.5%- efficient CdS/CdTe polycrystalline thin-film solar cell. *Proceedings of the 17th European Photovoltaic Solar Energy Conference, Munich, 22–26 October 2001*, 995–1000.
- [4] First Solar Sets Record for CdTe Solar PV Efficiency, 2016, <http://solarbuzz.com/industry-news/first-solar-sets-record-cdte-solar-pv-efficiency>.
- [5] T. M. Razykov, C. S. Ferekides, et al. Solar photovoltaic electricity: Current status and future prospects, *Solar Energy*. 85 (2011) 1580–1608.
- [6] Neelkanth G. Dhare. Scale-up issues of CIGS thin film PV modules. *Solar Energy Materials and Solar Cells Volume 95, Issue 1, January 2011, Pages 277–280*.



- [7] Wei Wang, Mark T, Winkler, Oki Gunawan, et al. Characteristics of CZTSSe Thin-Film Solar Cells with 12.6% Efficiency. *Adv. Energy Mater.* 2013, DOI: 10.1002/aenm.201301465.
- [8] Teodor K., Todorov, Jiang Tang, et al. Beyond 11% Efficiency: Characteristics of State-of-the-Art  $\text{Cu}_2\text{ZnSn}(\text{S},\text{Se})_2$  Solar Cells. *Adv. Energy Mater.* 2013, 3, 34–38.
- [9] Vasudeva Reddy, Minnam Reddy, Sreedevi Gedi, et al. Perspectives on SnSe-based thin film solar cells: a comprehensive review. *Journal of Materials Science: Materials in Electronics* June 2016, Volume 27, Issue 6, pp 5491-5508.
- [10] V. Kumar, Anita Sinha, et al. Concentration and temperature dependence of the energy gap in some binary and alloy semiconductors. *Infrared Physics & Technology* 69 (2015) 222–227.
- [11] R. Indirajith, T. P. Srinivasan K, et al. Synthesis, deposition and characterization of tin selenide thin films by thermal evaporation technique. *Current Applied Physics* 10 (2010) pp.1402-1406.
- [12] Nicolas D. Boscher, Claire J. et al. Atmospheric pressure chemical vapour deposition of SnSe and  $\text{SnSe}_2$  thin films on glass. *Thin Solid Films* 516 (2008) 4750–4757.
- [13] P. Suguna, D. Mangalaraj, S.A.K. Narayandass, P. Meena, *Phys. Stat. Sol. (A)* 115 (1996) 405.
- [14] N.R. Mathews. Electrodeposited tin selenide thin films for photovoltaic applications. *Solar Energy* 86 (2012) 1010–1016.
- [15] Optical and electrical properties of  $\text{SnSe}_2$  and SnSe thin films prepared by spray pyrolysis. D. Martínez-Escobar, Manoj Ramachandran, A. Sánchez-Juárez, Jorge Sergio Narro Rios. *Thin Solid Films* 535 (2013) 390–393.
- [16] S.J. Wakeham, G.J. Hawkins. Investigation of Cadmium Alternatives in Thin-Film Coatings, *Proc. of SPIE* Vol. 6286, 62860C, (2006).
- [17] Razykov T. M., Goswami Y., Kuchkarov K. M., et al. Electron microprobe X-ray spectral analysis of CMBD CdTe films of different composition. *Applied Solar Energy*, Volume 45, Issue 1, March 2009, Pages 48-50.
- [18] T. M. Razykov, C. S. Ferekides, K. M. Kouchkarov, et al. Effect of  $\text{CdCl}_2$  treatment on physical properties of CdTe films with different compositions fabricated by CMBD. *Applied Solar Energy*, 2015, Vol. 51, No. 4, pp. 314–318.
- [19] T. M. Razykov, K. M. Kouchkarov, Chris Ferekides, et al. Research of the Morphological and Structural Properties of CdTe Films Obtained by Chemical Molecular Beam Deposition for Thin Film Solar Cells. *Applied Solar Energy*, 2015, Vol. 51, No. 4, pp. 314–318.
- [20] T. M. Razykov. Chemical molecular beam deposition of II-VI binary and ternary compound films in gas flow. *Applied Surface Science*, 1991, v.48/49, N1, p.p.89-92.
- [21] Т. М. Разыков, К. М. Кучкаров. Структура изменения пленок CdTe и CdSe при химическом молекулярно-пучковом осаждении. // *Гелиотехника*. 2004. №4. стр.63-67.
- [22] Faheem K. Butt, Chuanbao Cao, Waheed S. Khan, Zulfiqar Ali, R. Ahmed, Faryal Idrees, Imran Aslam, M. Tanveer, Jili Li, Sher Zaman, Tariq Mahmood. Synthesis of highly pure single crystalline SnSe nanostructures by thermal evaporation and condensation route. *Materials Chemistry and Physics* 137 (2012) 565-570.
- [23] Deep Shikha, Vimal Mehta, Jeewan Sharma, et al. Effect of deposition temperature on structural, optical and electrical properties of nanocrystalline SnSe thin films. *J Mater Sci: Mater Electron* DOI 10.1007/s10854-016-5822-5 (2016).